Effect of synthesis parameters on cobalt ferrite saturation magnetization

IOP Conf. Series: Journal of Physics: Conf. Series **1123** (2018) 012017 doi:10.1088/1742-6596/1123/1/012017

Effect of synthesis parameters on cobalt ferrite saturation magnetization

H Soleimani*[1], N R Ahmad Latiff[1], H M Zaid[1], N Yahya[1], A R Sadrolhosseini[2], M Adil[1]

[1]Department of Fundamental and Applied Sciences, Universiti Teknologi PETRONAS, Bandar Seri Iskandar, 31750 Tronoh, Perak

[2]Departmen of Physics, Faculty of Science, Universiti Putra Malaysia, 43400 UPM Serdang, Malaysia, Malaysia,

hassan.soleimani@utp.edu.my

Abstract. Cobalt substituted magnetite, $Co_xFe_{1-x}Fe_2O_4$ was synthesized via co-precipitation method for $0.0 \leq x \leq 1.0$ and annealed in argon from 600 to 800°C to investigate the effect of synthesis parameters e.g. cation substitution and thermal treatment on its saturation magnetization. Particle size variation, crystallinity and cationic distribution between sublattices which resulted from the varying synthesis parameters are expected to alter the saturation magnetization of cobalt ferrite. Both thermal treatment and cation substitution are affecting the value of saturation magnetization. Correlation of microstructural properties with magnetization were analysed using TG-DTA, XRD, FTIR and VSM. Crystallinity, average crystallite size and lattice constant of the as-annealed samples is increasing with annealing temperature. The presence of maghemite and cobalt oxide as secondary phases have caused reduction in the saturation magnetization. Interestingly, increasing cobalt concentration in the samples has dramatically shifted the temperature at which magnetite transformed to maghemite. We have found that x=0.4 is the optimum cobalt ratio at which all reactants are converted into reaction product with no incomplete reactions that contribute to the formation of impurities. Preferential occupancy of Co^{2+} ions on the octahedral sites is evident in the FTIR spectra with intensified octahedral band splitting in the non-stoichiometric $Co_xFe_{1-x}Fe_2O_4$ ($0.2 \leq x \leq 0.8$), whereby the structures formed are in metastable state. It is also evident in the FTIR spectra that distinct absorption bands appeared only when the cations in both sites are well ordered. By substituting Co^{2+} ions, saturation magnetization keeps on increasing until x=0.4, and gradually reduced beyond that. Highest saturation magnetization (78.86 emu/g) was obtained in $Co_{0.4}Fe_{0.6}Fe_2O_4$ after annealing at 800°C. In conclusion, heat treatment and substitution of ferrous/ferric ions with cobalt of lower magnetic moment has amplified the super-exchange interaction between octahedral and tetrahedral sites in magnetite spinel structure for greater saturation magnetization.…

1. Introduction

Magnetite has been widely used for magnetic fluid research in enormous field *e.g.* magneto fluidics, flow control, heat generation, *etc*. due to its excellent magnetic properties [1]. Magnetic properties of magnetite nanoparticles strongly dependent on various factors *e.g.* synthesis route and particle size. In

magnetoviscosity, viscosity of magnetic particles suspended in a carrier fluid is tunable following the strength of the magnetic field applied and saturation magnetization of the particles [2]. The latter is highly sensitive to the crystallite size as spin disorder on the particles' surfaces escalated with the decrease in crystallite size [3]. Having stable configuration in ferrimagnetic spinel structure, magnetic properties of magnetite are affected by the inversion parameter which is attributed to the super exchange interaction between cations in tetrahedral and octahedral sites. Annealing temperature is one of the prime factors which effect the magnetization and cation distribution between two sites A and B [2, 3]. Via Mossbauer analysis, Chandra et. al (2017) has confirmed the migration of Co^{2+} ions to tetrahedral (A) sites as annealing temperature increases from 300 to 900°C, forcing Fe^{3+} ions to occupy the octahedral (B) sites and therefore intensify the A-B super-exchange interaction [2, 4]. Various studies on thermal kinetic of iron oxide have confirmed that phase transformation temperature for magnetite to transform to maghemite is around 450°C and beyond 600°C, hematite starts to form as it is the most stable polymorph of iron oxide [5, 6]. Interestingly, substitution of other elements into magnetite spinel structure has improved its thermal stability. Addition of 10% of cobalt ions into $Co_xFe_{3-x}O_4$ has improved the stability of magnetite up to 1000°C when heat treated in vacuum [8].

This work aims to investigate the effect of synthesis parameters e.g. cation substitution and thermal treatment on the magnitude of saturation magnetization of cobalt ferrite. Particle size variation, crystallinity and cationic distribution between sublattices which resulted from the varying synthesis parameters are expected to alter the saturation magnetization of cobalt ferrite.

2. Methodology

2.1. Synthesis of nanoparticles.

Co-precipitation method used in synthesizing cobalt ferrite nanoparticles has been adapted from literature [9]. Precursor solutions of iron (II) chloride, iron (II) chloride and cobalt (II) chloride were dissolved separately according to a pre-determined molar ratio in deionized water and then mixed together. A precipitant, 3.0 M sodium hydroxide was added to the salt solution dropwise until reaching pH 12. Subsequently, 1 mL of oleic acid was used as the chelating agent. The reaction was performed at 80°C for 2 hours with vigorous stirring. The precipitate prepared was then cooled to room temperature and centrifuged at 3000 rpm for 5 minutes to isolate it from the supernatant liquid. Subsequently, the black precipitate was washed with distilled water and acetone several times and was then dried for 24 hours. Thus, the samples of as-precipitated $Co_xFe_{1-x}Fe_2O_4$ were further calcined at 600, 700 and 800°C for 2 hours at a heating rate of 10 °C/min in argon stream.

2.2. Structural and Magnetic Properties Characterization.

The structural properties of the sintered samples were characterized by X-ray diffractometer (XRD). Magnetic properties were measured using vibrating sample magnetometer (VSM) up to a maximum applied field of 20,000 Oe at room temperature. FTIR transmission spectra were taken on Perkin Elmer Spectrum BX model Infrared Spectrophotometer from 200 to 4000 cm^{-1}. The thermogravimetric analysis (TG) and corresponding differential thermal analysis (DTA) of the as-precipitated $Co_xFe_{1-x}Fe_2O_4$ nanoparticles have been carried out in argon at the rate of 10°C/min up to 1100°C.

3. Results and Discussion

The TG-DTA thermograms (Figure 1) provide useful information regarding thermal behaviour of the samples e.g. the temperature of solvent decomposition, phase transformation and isochemical transformation (i.e. cations redistribution between the octahedral and tetrahedral sites) [10]. Three-stage decomposition is observed during heating from 25 to 1100°C. Different thermal profiles were exhibited by samples of various Co^{2+} ratio. However, all samples show similar thermal profile below 100°C,

whereby the first stage mass loss is associated to the removal of moisture from the samples with around 5% mass loss. This is supported by an endothermic peak presents around 70°C which attributed to the vaporization process of the hydroxyl group [11].

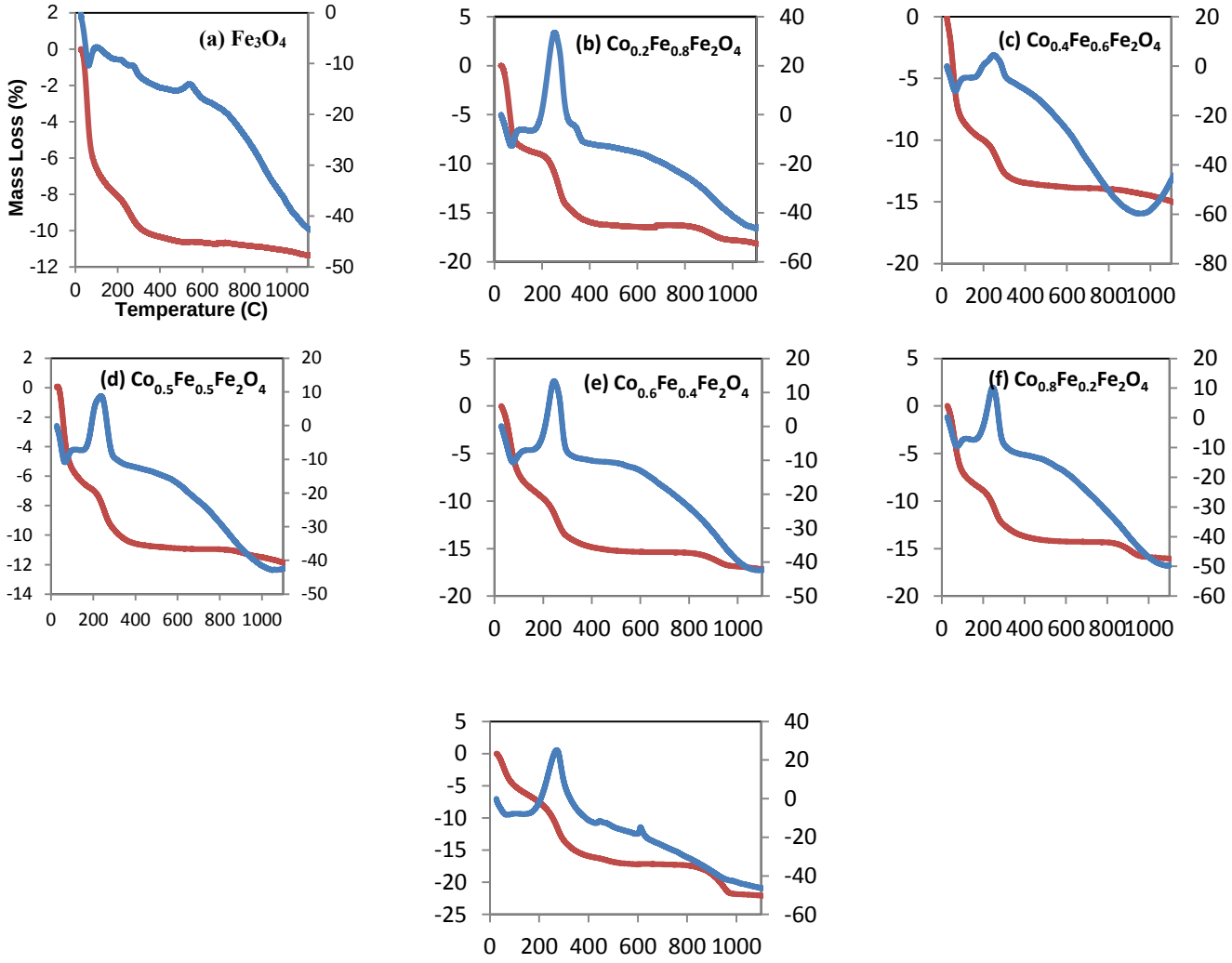

Figure 1. TG-DTA thermograms of the as-precipitated $Co_xFe_{1-x}Fe_2O_4$ samples at varying cobalt concentration

Interestingly, we observed that a major exothermic peak around 250°C is present in the DTA thermogram of all samples, with exception for Fe_3O_4 (Figure 1a). Instead, two small bumps appear at 230 and 280°C, with around 2% mass loss is due to the dissociation of weakly bounded or free oleate molecules from the oleic acid used as surfactant [12]. Another exothermic peak with no mass loss appeared around 570°C is attributed to the phase transformation of maghemite to hematite [7]. Since TGA is not sufficient to detect polymorphous transformations as they do not involve any mass change, DTA can be used to observe the heat flow by differentiating the heat evolved when exothermic or endothermic events occur [13]. Beyond 600°C, insignificant mass loss with no variation in heat flow is observed, denoting the thermal decomposition of Fe_3O_4 sample has been completed.

When doped with Co^{2+}, changes in the thermograms are also observed. With addition of foreign elements into magnetite structure, the conversion of maghemite to hematite is shifted to higher temperature, making it more stable at elevated temperature [7]. When we look closely to thermograms of other compositions (Figure 1b-1f), two noticeable differences in terms of exothermic peaks

appearance can be listed. Firstly, an exothermic peak around 250-270°C with mass loss around 3-5% appeared in all samples for x>0. This peak is associated with the decomposition of CoO(OH) to Co_3O_4, which existed due to the incomplete reaction during precipitation synthesis[14]. Secondly, no maghemite to hematite conversion peak was observed for intermediate composition ($0.2 \leq x \leq 0.8$), justifying that only maghemite phase is present in the sample after being annealed up to 800°C. However, for x=1, the maghemite to hematite peak reappear at 634°C, in agreement to other findings which reported shifting of phase conversion to higher temperature [7], [8]. Final mass loss observed around 970-980°C for x>0 is attributed to the decomposition of Co_3O_4 to CoO, which explains the existence of secondary phases in XRD patterns that will be discussed in the next subsections [14].

Putting a material under thermal treatment is a way to improve its properties. For instance, saturation magnetization of a magnetic material increases with increase in particle size and crystallinity. X-ray diffraction patterns of cobalt ferrite samples at various cobalt concentration and annealing temperature are providing information on the crystallinity and purity of the as-annealed samples (Figure 2). Seven characteristics peaks of spinel cubic structure (Fd-3m) were reflected from crystal planes corresponding to (220), (311), (222), (400), (422), (511) and (440) which are indexed to the standard cobalt ferrite (ICSD 16-0059).

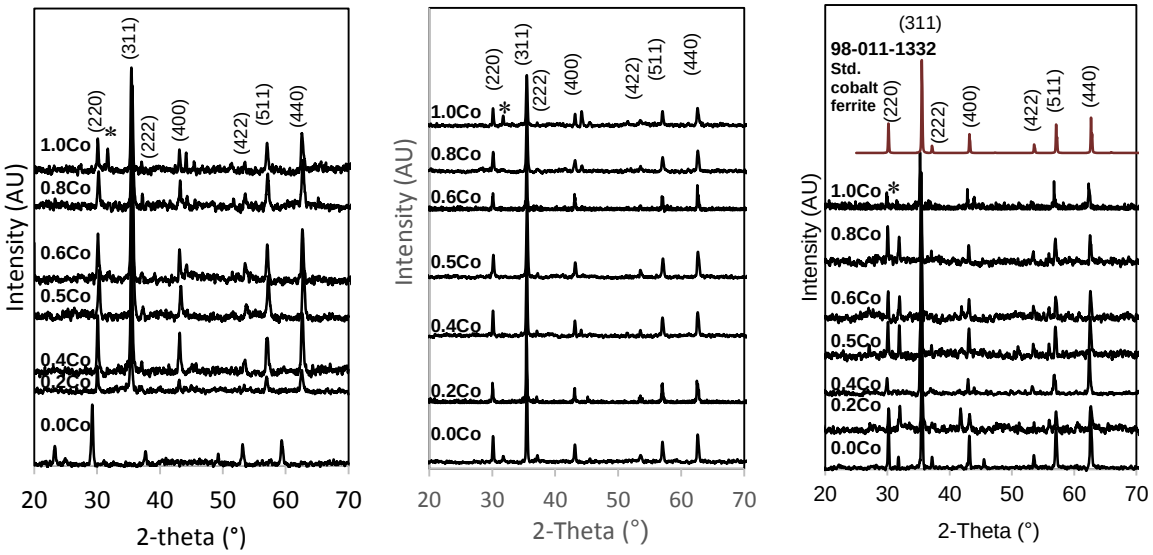

(a) (b) (c)

Figure 2. Diffraction patterns of $Co_xFe_{1-x}Fe_2O_4$, for $0 \leq x \leq 1$ at various annealing temperature (a) 600°C, (b) 700°C and (c) 800°C

However, additional peaks appear consistently in almost all samples at similar Bragg angle which were indexed as maghemite, γ-Fe_2O_3 (PDF 39-1346) [15]. The presence of maghemite is anticipated as annealing the samples at temperatures higher than 180°C will caused rapid oxidation of Fe^{2+} to Fe^{3+} which promotes formation of maghemite [16]. This effect is also observed in this work when the annealing temperature increases from 600 to 800°C (Figure 2 (a), (b) and (c)), the peak intensity of maghemite gets higher. However, transformation kinetics of iron oxide with temperature shows that formation of maghemite is not possible in this temperature range [17]. Annealing of magnetite at various temperature has shown that conversion of magnetite to hematite started at 650 °C and was fully complete at 750 °C without the formation of maghemite [17]. This finding is puzzling as no hematite is detected from the diffraction pattern analysis.

Interestingly, Pati et al.(2012) demonstrated that doping cobalt ions into magnetite structure at various Co^{2+} ratio and annealing temperature has dramatically increases the phase transformation temperature of magnetite [7]. From thermal analysis (TG-DTA) discussed earlier, it is confirmed that

maghemite to hematite conversion shifted from 570°C (Fe_3O_4) to 634°C ($CoFe_2O_4$) and no conversion in the intermediate composition. As Co_3O_4 only decomposes to CoO beyond 970°C, cobalt oxide will remain in the sample within annealing temperature applied in this work. In other work, increasing the annealing temperature to 1000°C has successfully produced single phase cobalt ferrite, which is also in agreement to the TG-DTA discussed earlier [18]. When growth of larger particle due to extreme temperature exposure is undesirable, formation of secondary phases e.g. maghemite and goethite due to oxidation of Fe^{2+} to Fe^{3+} should be suppressed from the beginning, which is by careful control of initial reaction pH and the ideal ratio of ferrous and ferric ions [16]. To get ideal Fe^{2+}/Fe^{3+}, ratio of 1:2 is optimized for reaction in inert environment and 2:3 for reaction conducted in ambient condition [16].

Major diffraction peak (311) is used to estimate the crystallite sizes of cobalt ferrite samples via typical Scherrer equation. Variation of crystallite size and lattice constant with cobalt concentration is shown in Figure 3. At a fixed annealing temperature, lattice constant is decreasing with increase in cobalt concentration due to the difference in the ionic radii [19]. When larger Fe^{2+} (0.074 nm) being substituted by Co^{2+} (0.068 nm), lattice contraction occurs and reduction in lattice constant is observed. Meanwhile, different trend is observed when annealing temperature is varied at a fixed cobalt concentration, whereby both lattice constant and average crystallite size increase with temperature.

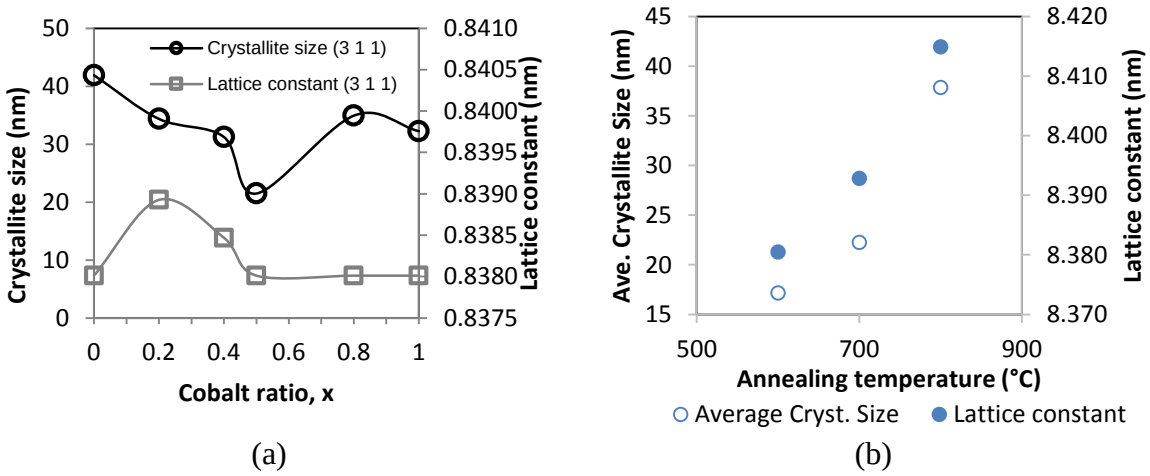

(a) (b)

Figure 3. Evolution of crystallite size and lattice constant of cobalt ferrite at (a) various cobalt cation concentration (fixed temperature) and (b) various annealing temperature

Qualitative analysis of the cationic distribution may be deduced using FTIR spectra since the absorption bands position depends on several factors e.g. bond type and strength, coordination and the nature of ions involved [20]. Variation of vibrational band for metal-oxygen bonds has been observed due to the presence of more than one type of cation e.g. Fe-O, Co-O. Different bond lengths caused the variation in the band positions as shorter bonds vibrate/oscillate at higher frequencies that the long ones. In normal spinel, two distinct vibrational bands which attributed to the bond vibrations in tetrahedral and octahedral sites are clearly visible [20]. However, in the case of mixed and inverse spinel, broadening and splitting of tetrahedral and octahedral bands into multiple bands occur due to the presence of more than one type of cations in a respective sublattice or similar type of cations co-existed in both sites [20].

Formation of spinel ferrites can be validated through FTIR spectra by observing the position of absorption bands around 300 to 600 cm^{-1}. The high frequency band υ_1, which is generated by the stretching vibration of the metal-oxygen bonds in tetrahedral sites can be detected around 550–590 cm^{-1}. Meanwhile, absorption band due to metal–oxygen vibrations in the octahedral sites (υ_2) ranging from 350–400 cm^{-1} [21]. From Figure 4, υ_1 positions appear consistently around 560 to 570 cm^{-1}, with no significant dependence on the cobalt concentration increment. While intensity of υ_1 does increases with cobalt concentration, it is also discovered that splitting and broadening of the υ_2 intensified as a result of

cationic redistribution between the two sublattices [22]. It is safe to conclude that in this work, Co^{2+} ions preferentially occupy the octahedral sites and co-exist with the Fe^{3+} ions which justified the band splitting into several sub-bands and appearance of shoulders in the broadened region [15, 16]. Similar observation has been reported with cobalt ferrite synthesized via co-precipitation method [24]. Since none of the band splitting is observed around designated tetrahedral band position, forced migration of Fe^{3+} ions into the tetrahedral sites are boosting its population in it, causing the band intensity to increase as Co^{2+} increases[20].

It is also evident in the FTIR spectra that distinct absorption bands appeared only when the cations in both sites are well ordered [23]. For the pure magnetite and cobalt ferrite samples, both characteristic bands of spinel are observed along with an ultralow frequency band around 250–320 cm^{-1} which generated from the stretching vibrations of Fe^{2+} ions [23]. In the samples of intermediate composition ($0.2 \leq x \leq 0.8$), band splitting is observed and gradually smeared out with increase in x values. Conversely, annealing the samples from 600 to 800 °C does change the crystallinity and cation distribution in cobalt ferrite. Broadening of octahedral bands along with smearing out of the split bands and shoulders is correlated with the crystallinity improvement resulting from increase in annealing temperature [25].

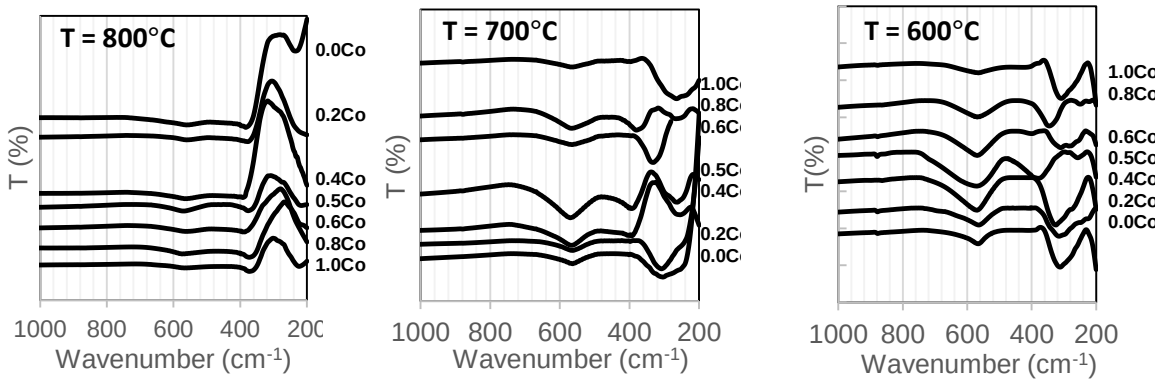

(a) (b) (c)

Figure 4. FTIR spectra of $Co_xFe_{1-x}Fe_2O_4$, for $0 \leq x \leq 1$ post-annealing at (a) 800°C, (b) 700°C and (c) 600° in argon for 2 hours

The magnetization (M-H) loops of $Co_xFe_{1-x}Fe_2O_4$, for all *x* values post annealed at 800°C are given in Figure 5. Only one temperature is discussed in this section as magnetization profile of all samples at other temperatures shows almost similar behavior. Saturation magnetization of a ferrimagnetic material is generally governed by the exchange interaction between Fe^{2+}, Fe^{3+} and Co^{2+} ions in tetrahedral and octahedral sublattices, increase in particle size from heat treatment and the presence of impurities or secondary phases [6, 17, 19, 24, 25]. The effect of cation distribution on the magnetization of $Co_xFe_{1-x}Fe_2O_4$ is shown in Figure 5. Magnetic behavior of the samples changes with varying Co^{2+} concentration. At x=0, no cobalt was present and the M-H loop resembling magnetite, showing paramagnetic curve with very low coercivity (~100 Oe) but slightly lower saturation magnetization to that of magnetite reported in literatures (52.54 emu/g). With increasing temperature (Figure 6), slight changes in the saturation magnetization and coercivity were found in coordination with polymorphous transformation of magnetite as described in TG-DTA analysis. Paramagnetic maghemite phase gives high saturation magnetization for samples annealed at 600 and 700°C, while the co-existence of maghemite and hematite beyond 700°C potentially explains the slight decrease in saturation magnetization [17].

Previous studies has reported the occupation of Co^{2+} ions in both sublattices, but with preference in octahedral sites for bulk ferrites [28], [29]. From FTIR analysis discussed in the previous section, it is evident that Co^{2+} ions in $Co_xFe_{1-x}Fe_2O_4$, have strong tendency to occupy the octahedral sites. For $0.2 \leq x \leq 0.8$, gradual change from soft to hard ferromagnetic is observed, which is defined by the

coercivity values and the width of hysteresis curves (Figure 5). Saturation magnetization increases with cobalt doping up to x=0.4, before gradually decrease upon cobalt addition up to x=1.0.

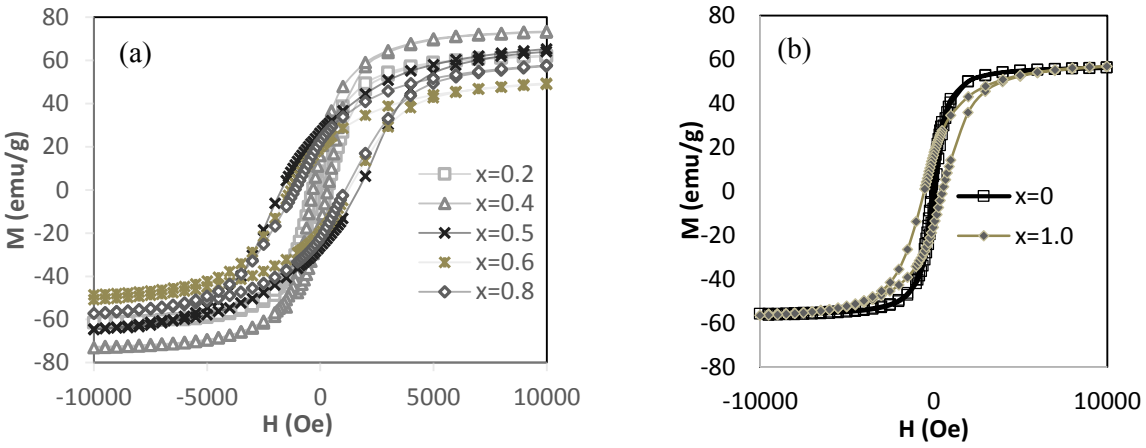

Figure 5. Magnetization M-H loops of $Co_xFe_{1-x}Fe_2O_4$, for (a) $0.2 \leq x \leq 0.8$ and (b) x=0,1.0 at 800°C

Presence of impurities affect magnetization of $Co_xFe_{1-x}Fe_2O_4$. A direct correlation between the presence of impurities or multiphase cobalt ferrite and the magnitude of saturation magnetization could be observed [30]. As shown in the XRD patterns, presence of maghemite in the final product is expected to cause reduction in the saturation magnetization. No peak of maghemite was detected which explains higher magnitude of saturation magnetization when compared with other samples annealed at 800°C.

Varying the annealing temperature does change the magnetic properties of the samples. It is generally known that particle size is the governing parameter in determining the magnetic properties of materials. As the temperature increases from 600 to 800°C, saturation magnetization of sample x=0.4 increases from 39 emu/g to 78.86 emu/g. From XRD analysis, particle size gets larger with increasing annealing temperature. With the decreasing contribution from the surface shell with increasing particle size, magnetization of samples improved as annealing temperature increases [31].

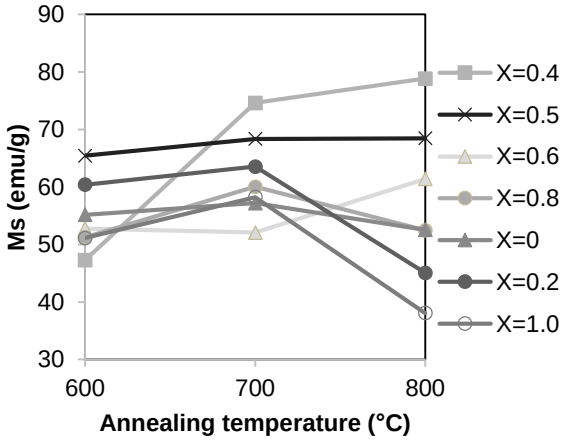

T

Figure 6. Saturation magnetization of $Co_xFe_{1-x}Fe_2O_4$ for all x values as a function of annealing temperatures

4. Conclusion

Saturation magnetization of $Co_xFe_{1-x}Fe_2O_4$ is highly affected by the heat treatment and cobalt ions substitution. Post annealing at 800°C results in particle size increase for highest magnitude of saturation

magnetization at x=0.4. We have found that *x*=0.4 is the optimum cobalt ratio at which all reactants are converted into reaction product with no incomplete reactions that contribute to the formation of impurities. Preferential occupancy of cobalt ions into octahedral sites is causing the increase of saturation magnetization with cobalt doping up to x=0.4 and gradually decreases beyond that as the lower magnetic moment of cobalt ion is reducing the exchange interaction between octahedral and tetrahedral sites.

Acknowledgement
The authors would like to thank Universiti Teknologi PETRONAS and Petroliam Nasional Berhad (PETRONAS) for providing research grants 0153AA-E05 (YUTP) and 0153CB-010(GR&T).

References

[1] Soleimani H, Latiff NRA, Yahya N, Sabet M, Khodapanah L, Kozlowski G, Chuan LK, and Guan BH 2016 *J. Nano Res.* **38** 40–6
[2] Zaid HM, Wan Azahar WA, Soleimani H, Ahmad Latiff NR, Shafie A, Lee KC, and Beh HG 2014, *J. Nano Res.* **29** 115–20
[3] Mascolo MC, Pei Y, and Ring TA 2013 *Materials* **6** 5549–67
[4] Chandra G, Srivastava RC, Reddy VR, and Agrawal H 2017 *J. Magn. Magn. Mater.* **427** 225–9
[5] El-Okr MM, Salem MA, Salim MS, El-Okr RM, Ashoush M, and Talaat HM 2011 *J. Magn. Magn. Mater.* **323** 920–6
[6] Nadeem K, Rahman S, and Mumtaz M 2015 *Prog. Nat. Sci. Mater. Int.* **25** 111–6
[7] Pati SS, Gopinath S, Panneerselvam G, Antony MP, and Philip J 2012 *J. Appl. Phys.* **112**
[8] Anjum S, Tufail R, Rashid K, Zia R, and Riaz S 2017 *J. Magn. Magn. Mater.* **432** 198–207
[9] Habibi MH and Parhizkar HJ 2014 *Spectrochim. Acta Part A Mol. Biomol. Spectrosc.* **127** 102–6
[10] Rana S, Philip J and Raj B 2010 *Mater. Chem. Phys.* **124** 264–9
[11] Aghav PS, Dhage VN, Mane ML, Shengule DR, Dorik RG, and Jadhav KM 2011 *Phys. B* **406** 4350–54
[12] Herrera AP, Polo-Corrales L, Chavez E, Cabarcas-Bolivar J, Uwakweh ONC and Rinaldi C 2013 *J. Magn. Magn. Mater.* **328** 41–52
[13] MacHala L, Tuček J, and Zbořil R 2011 *Chem. Mater.* **23** 3255–72
[14] Yang J, Liu H, Martens WN and Frost RL 2010 *J. Phys. Chem. C* **114** 111–9
[15] Kim W, Suh CY, Cho, Roh KM, Kwon H, Song K, and Shon IJ 2012 *Talanta* **94** 348–52
[16] Gnanaprakash G, Mahadevan S, Jayakumar T, Kalyanasundaram P, Philip J and Raj B 2007 *Mater. Chem. Phys.***103** 168–75
[17] Jafari A, Farjami S, Salouti M and Boustani K 2015 *J. Magn. Magn. Mater.***379** 305–312
[18] Mohamed RM, Rashad MM, F. Haraz FA and Sigmund W *J. Magn. Magn. Mater.* **322** 2058–64
[19] Babukutty B, Nair SS and Kalarikkal N 2017 *Mater. Res. Express* **4**
[20] Rathod V, Anupama AV, Kumar RV, Jali VM and Sahoo B 2017 *Vib. Spectrosc.* **92** 267–272
[21] Saffari F, Kamelin P, Rahimi M, Ahmadvand H and Salamati H 2015 *Ceram. Int.* **41** 7352–58
[22] Kumar L, Kumar P and Kar M 2013 *J. Alloys Compd.* **551** 72–81
[23] Rathod V, Anupama AV, Jali VM, Hiremath VA and Sahoo B 2017 *Ceram. Int.* **43** 14431–40
[24] Baraliya JD and Joshi HH 2014 *Vib. Spectrosc.* **74** 75–80
[25] Kumar L, Kumar P, Narayan A and Kar M 2013 *Int. Nano Lett.* **3** 8
[26] Yadav SP, Shinde SS, Bhatt P, Meena SS and Rajpure KY 2015 *J. Alloys Compd.* **646** 550–6
[27] Ati AA, Othaman Z and Samavati A 2013 *J. Mol. Struct.* **1052** 177–182
[28] Ajroudi L, Mliki, Bessais L, Madigou V, Villain S and Leroux C 2014 *Mater. Res. Bull.* **59** 49–58
[29] Safi R, Ghasemi A and Shoja-Razavi R 2016 *Ceram. Int.* **42** 15818–25

[30] Soleimani H, Latiff NRA, Yahya N, Zaid HM, Sabet M, Beh HG, and Lee KC 2014 *J. Nano Res.* **29** 105-13
[31] Swatsitang E, Phokha S, Hunpratub S, Usher B, Bootchanont A, Maensiri S and Chindaprasirt P 2016 *J. Alloys Compd.* **664** 792–7